Earthquake Geotechnical Engineering for Protection and Development of Environment and Constructions – Silvestri & Moraci (Eds)

ISBN 978-0-367-14328-2

Analysis of partially saturated liquefiable soil through strain space multiple mechanism model

S. Iai
FLIP Consortium, Kyoto, Japan

K. Ueda
Kyoto University, Kyoto, Japan

ABSTRACT: This paper presents a new formulation of governing equation of three phase medium, consisting of solid skeleton, gas and water through a generalized fluid vector and presents two examples of application to partially saturated liquefiable soil. One example is the application to horizontally layered partially saturated liquefiable ground. In particular, behavior of soil above the ground water is discussed in detail in this example, including change in degree of saturation due to pore water seepage flow above the ground water table. The other example is on an embankment retaining water in one side, where initially seepage flow and phreatic line analysis is presented as initial seepage and gravity analysis, and then earthquake shaking is applied at the base to discuss the behavior of partially saturated embankment.

1 INTRODUCTION

The strain space multiple mechanism model (Iai et al., 2011) has been widely used for liquefaction induced damage to various soil-structure systems. Through the development of this model, application of this model has been limited for fully saturated or fully dried state of soils. In the present paper, a new development in described by extending the application of strain space multiple mechanism model into partially saturated soil.

The governing equations of saturated soil, if the acceleration of pore water relative to that of solid skeleton is negligibly small, can be written in terms of equilibrium equation of soil element, consisting of solid skeleton and pore water, and mass balance equation of pore water flowing through pores, or voids, of porous material as follows (Zienkiewicz and Bettess, 1982):

Equilibrium:

$$\mathrm{div}\sigma + \rho\mathbf{g} = \rho\ddot{\mathbf{u}} \tag{1}$$

Mass balance of pore water:

$$n\dot{p}/K_{\mathrm{f}} + \mathrm{div}(\underline{\mathbf{u}}) = -\mathrm{div}(\mathbf{k}[-\mathrm{grad}(p) + \rho_{\mathrm{f}}\mathbf{g} - \rho_{\mathrm{f}}\ddot{\mathbf{u}}]) \tag{2}$$

where σ denotes total stress tensor (extension positive), ρdenotes density, $\mathbf{g}$ denotes acceleration of gravity vector, $\mathbf{u}$ denotes displacement vector, n denotes porosity, p denotes pore water pressure (compression positive), $\mathbf{k}$ denotes coefficient of permeability tensor, and ρ_{f} denotes density of water. By writing the total stress in Eq.(1) as a summation of effective stress and pore water pressure as $\sigma = \sigma' - \mathbf{m}p$, where $\mathbf{m}$ denotes second order unit tensor consisting of components δ_{ij}, the governing equations of saturated soil as two phase medium is written in discretized form with the variables of nodal displacement vector $\underline{u}$ and pore water pressure vector $\underline{p}$ through the typical finite element formulation as follows (Ozutsumi, 2003):

$$\int_{\Omega} \mathbf{B}^{\mathrm{T}} \hat{\sigma}' \mathrm{d}v - \mathbf{Q}\underline{\mathbf{p}} + \mathbf{M}(g\underline{I}_{\mathrm{v}} + \underline{\ddot{u}}) - \int_{\partial\Omega_\sigma} \mathbf{H}^{\mathrm{T}} \bar{\mathbf{t}} \mathrm{d}s = 0 \tag{3}$$

$$\mathbf{G}\underline{p} + \mathbf{R}\underline{\dot{p}} = \int_{\partial\Omega_{\mathbf{q}_\mathrm{f}}} \hat{\mathbf{H}}^{\mathrm{T}} \bar{\mathbf{q}} \mathrm{d}s - \mathbf{Q}^{\mathrm{T}} \underline{\dot{u}} - \hat{\mathbf{M}}(g\underline{I}_{\mathrm{v}} + \underline{\ddot{u}}) \tag{4}$$

where $\hat{\sigma}'$ denotes effective stress vector in vector-matrix representation and symbols with capital bold letters such as **B**, etc. represent discretized matrices of differential operators such as div, etc. in Eqs.(1) and (2).

Generalization into three phase medium briefly discussed in the following (Sections 2 through 4) is based on Iai (2018).

2 GOVERNING EQUATIONS OF PARTIALLY SATURATED SOIL

Partially saturated soil is idealized as porous media of solid skeleton with two kinds of pores; one for fluid (f), the other for air (a). These pores are assumed unconnected with each other, i. e. there is no interaction between the flows of fluid and air (Borja, 2004). Partially saturated soil with degree of saturation S_r and porosity n has volume of fluid nS_r and that of air $n(1 - S_\mathrm{r})$. If there is no change in degree of saturation, the governing equations of partially saturated soil is obtained by modifying Eq.(2) in accordance with the volumes of fluid and air by multiplication of S_r and $(1 - S_\mathrm{r})$ in the left hand side of the equation together with the introducing bulk moduli, coefficient of permeability, and densities of fluid and air, respectively. In general there is change in degree of saturation and, in this general condition of partially saturated soil of three phase medium, adding the term for representing the volume change of fluid and air (i. e. time derivative of volume) to these mass balance equations will lead to the following generalized mass balance equation:

Mass balance of fluid:

$$n\dot{S}_\mathrm{r} + nS_\mathrm{r}\dot{p}_\mathrm{f}/K_\mathrm{f} + S_\mathrm{r}\mathrm{div}(\underline{\mathbf{u}}) = -\mathrm{div}\big(\mathbf{k}^\mathrm{f}[-\mathrm{grad}(p_\mathrm{f}) + \rho_\mathrm{f}\mathbf{g} - \rho_\mathrm{f}\ddot{\mathbf{u}}]\big) \tag{5}$$

Mass balance of air:

$$-n\dot{S}_\mathrm{r} + n(1 - S_\mathrm{r})\dot{p}_\mathrm{a}/K_\mathrm{a} + (1 - S_\mathrm{r})\mathrm{div}(\underline{\mathbf{u}}) = -\mathrm{div}(\mathbf{k}^\mathrm{a}[-\mathrm{grad}(p_\mathrm{a}) + \rho_\mathrm{a}\mathbf{g} - \rho_\mathrm{a}\ddot{\mathbf{u}}]) \tag{6}$$

The change in the degree of saturation can be written as a function of suction s in terms of tangential slope of soil-water retention characteristic curve as

$$\dot{S}_\mathrm{r} = \frac{\partial S_\mathrm{r}}{\partial s}\dot{s} = \chi(\dot{p}a - \dot{p}f) \quad , \quad s = pa - pa \tag{7}$$

Substitution of this term into Eqs.(5) and (6) yields the governing equations for partially saturated soil together with Eq.(1).

The effective stress of partially saturated soil can be defined based on a representative pore pressure (a pressure of a mixture of fluid and air filling void of soil) p^* as follows:

$$\sigma = \sigma' - \mathbf{m}p^* \tag{8}$$

Two definitions are available of the representative pore pressure; one is a weighted average of pressures of fluid and air consistent with the volume ratio in accordance with the degree of saturation S_r, the other is a weighted average in accordance with the effective degree of saturation S_r^* (Ohno et al., 2006), defined as follows:

$$p^* = S_\mathrm{r}p_\mathrm{f} + (1 - S_\mathrm{r})p_\mathrm{a} \quad or \quad p^* = S_\mathrm{e}p_\mathrm{f} + (1 - S_\mathrm{e})p_\mathrm{a}\ , \quad S_\mathrm{e} = \frac{S_\mathrm{r} - S_\mathrm{rn}}{S_\mathrm{rx} - S_\mathrm{rn}} \tag{9}$$

where S_rx denotes degree of saturation when suction becomes $s = 0$ during wetting process, and S_rn denotes degree of saturation when suction reaches $s = \infty$ during drying process.

3 INTRODUCING GENERALIZED FLUID VECTOR (THREE PHASE MEDIUM)

Substitution of Eq.(8) to Eq.(1) yields the equilibrium equation for partially saturated soil written in terms of effective stress, fluid and air pressures. In addition to this equilibrium equation, mass balance equations of fluid and air in Eqs.(5) through (7) can be discretized as:

$$\int_{\Omega} \mathbf{B}^{\mathrm{T}}\hat{\sigma}'\mathrm{d}v - \mathbf{Q}^{\mathrm{f}*}\underline{\mathbf{p}}_{\mathrm{f}} - \mathbf{Q}^{\mathrm{a}*}\underline{\mathbf{p}}_{\mathrm{a}} + \mathbf{M}(g\underline{\mathbf{I}}_{\mathrm{v}} + \underline{\ddot{\mathbf{u}}}) - \int_{\partial\Omega_{\sigma}} \mathbf{H}^{\mathrm{T}}\bar{\mathbf{t}}\mathrm{d}s = 0 \tag{10}$$

$$\mathbf{G}^{\mathrm{f}}\underline{\mathbf{p}}_{\mathrm{f}} + \mathbf{R}^{\mathrm{f}}\underline{\dot{\mathbf{p}}}_{\mathrm{f}} + \mathbf{R}^{\mathrm{fa}}\underline{\dot{\mathbf{p}}}_{\mathrm{a}} = \int_{\partial\Omega_{q_{\mathrm{f}}}} \hat{\mathbf{H}}^{\mathrm{T}}\bar{\mathbf{q}}_{\mathrm{f}}\mathrm{d}s - \mathbf{Q}^{\mathrm{f}^{\mathrm{T}}}\underline{\dot{\mathbf{u}}} - \hat{\mathbf{M}}^{\mathrm{f}}(g\underline{\mathbf{I}}_{\mathrm{v}} + \underline{\ddot{\mathbf{u}}}) \tag{11}$$

$$\mathbf{G}^{\mathrm{a}}\underline{\mathbf{p}}_{\mathrm{a}} + \mathbf{R}^{\mathrm{a}}\underline{\dot{\mathbf{p}}}_{\mathrm{a}} + \mathbf{R}^{\mathrm{af}}\underline{\dot{\mathbf{p}}}_{\mathrm{f}} = \int_{\partial\Omega_{q_{\mathrm{a}}}} \hat{\mathbf{H}}^{\mathrm{T}}\bar{\mathbf{q}}_{\mathrm{a}}\mathrm{d}s - \mathbf{Q}^{\mathrm{a}^{\mathrm{T}}}\underline{\dot{\mathbf{u}}} - \hat{\mathbf{M}}^{\mathrm{a}}(g\underline{\mathbf{I}}_{\mathrm{v}} + \underline{\ddot{\mathbf{u}}}) \tag{12}$$

Generalized fluid vectors introduced in this paper are defined by combining the degree of freedoms of variables of fluid and air pressures and boundary inflows of fluid and air as

$$\underline{\mathbf{p}} = \begin{bmatrix} \underline{\mathbf{p}}_{\mathrm{f}} \\ \underline{\mathbf{p}}_{\mathrm{a}} \end{bmatrix}, \bar{\mathbf{q}} = \begin{bmatrix} \bar{\mathbf{q}}_{\mathrm{f}} \\ \bar{\mathbf{q}}_{\mathrm{a}} \end{bmatrix} \tag{13}$$

In accordance with introduction of the generalized fluid vectors, the matrices in Eqs.(10) through (12) can be also combined into generalized matrices as

$$\mathbf{Q}^{*} = \begin{bmatrix} \mathbf{Q}^{\mathrm{f}*} & \mathbf{Q}^{\mathrm{a}*} \end{bmatrix}, \mathbf{G} = \begin{bmatrix} \mathbf{G}^{\mathrm{f}} & \mathbf{0} \\ \mathbf{0} & \mathbf{G}^{\mathrm{a}} \end{bmatrix}, \mathbf{R} = \begin{bmatrix} \mathbf{R}^{\mathrm{f}} & \mathbf{R}^{\mathrm{fa}} \\ \mathbf{R}^{\mathrm{af}} & \mathbf{R}^{\mathrm{a}} \end{bmatrix}, \hat{\mathbf{M}} = \begin{bmatrix} \hat{\mathbf{M}}^{\mathrm{f}} \\ \hat{\mathbf{M}}^{\mathrm{a}} \end{bmatrix}, \overline{\overline{\hat{\mathbf{H}}}} = \begin{bmatrix} \hat{\mathbf{H}} & \mathbf{0} \\ \mathbf{0} & \hat{\mathbf{H}} \end{bmatrix} \tag{14}$$

By using these generalized fluid vectors and matrices, the discretized governing equations in Eqs.(10) through (12) are reduced the same form of the governing equations of fully saturated soil (two phase medium) shown in Eqs.(3) and (4), given by

$$\int_{\Omega} \mathbf{B}^{\mathrm{T}}\hat{\sigma}\prime\mathrm{d}v - \mathbf{Q}^{*}\underline{p} + \mathbf{M}(g\underline{I}_{\mathrm{v}} + \underline{\ddot{\mathbf{u}}}) - \int_{\partial\Omega_{\sigma}} \mathbf{H}^{\mathrm{T}}\bar{\mathbf{t}}\mathrm{d}s = 0 \tag{15}$$

$$\mathbf{G}\underline{\mathbf{p}} + \mathbf{R}\underline{\dot{\mathbf{p}}} = \int_{\partial\Omega_{q}} \overline{\overline{\hat{\mathbf{H}}}}^{T}\bar{\mathbf{q}}\mathrm{d}s - \mathbf{Q}^{\mathrm{T}}\underline{\dot{\mathbf{u}}} - \hat{\mathbf{M}}(g\underline{\mathbf{I}}_{v} + \underline{\ddot{\mathbf{u}}}) \tag{16}$$

The matrix **Q** representing the coupling of solid skeleton displacement and pore fluid pressure in Eq.(3) for fully saturated soil is replaced by $\mathbf{Q}^*$ for partially saturated soil in Eq.(15) in accordance with the definition of representative pore pressure for defining the effective stress of partially saturated soil in Eq.(9). The integral over the fluid boundary in Eq.(16) is symbolic and actually implemented separately for fluid and air boundaries as shown for the integrals in Eqs.(11) and (12).

Description of the generalized vectors and matrices in Eqs.(13) and (14) adopts the components of the vectors in the order of the degree of freedom of fluid pressure first followed by the degree of freedom of air pressure. This order of components is actually not adopted. The actual order of the components of generalized fluid vector is defined by the order of nodes with each node having two degrees of freedom consisting of fluid and air pressures. The orders of the components of the matrices in Eq.(14) are defined accordingly.

The formulation of the partially saturated soil as three phase medium presented in Eqs.(15) and (16) has the advantage in the simplicity in the structure of computer programming of partially saturated soil. This formulation has also advantage in its generality to expand the framework of the theory to generalized fluid having more than two degrees of freedom, such as the porous material with more than one type of fluid and gas, such as water, air, oil, and natural gas, all inclusive.

4 SOIL-WATER RETENTION CHARACTERISTICS AND PERMEABILITY

Soil-water retention characteristics assumed for this study is based on van Genuchten (1980) as

$$S_r = (S_{rx} - S_m)[1 + s/s_a)^{n_f}]^{-m_f} + S_m \tag{17}$$

where the parameter s_a is identified as the suction at the degree of saturation given by S_r=(S_{rx} +S_{rn})/2 if m_f=1. In particular, subscripts U and L are added for the parameters s_a and n_f to indicate upper and lower limiting curves for drying and wetting processes, respectively (U and L curves in Figure 1 with parameters in Table 1). Whereas these limiting curves can be used as an option for setting up initial conditions for earthquake response analysis stage, this study also allows the use of generalized curve (M curve located between U and L curves in Figure 1) in the initial gravity analysis stage of soil-structure systems for setting up initial conditions for earthquake response analysis stage. This middle curve is defined by projection of upper and lower limiting curves and specified by a pseudo reversal point with degree of saturation S_{ri} and suction s_i, both of which are often specified as initial condition for earthquake response analysis of partially saturated soil.

Hysteretic behavior of soil in soil-water retention characteristics is idealized by projection of upper or lower limiting curve for drying or wetting process beginning from a reversal point within these curves. An example of hysteretic curve beginning from point A, going through point B for wetting process due to inflow of pore water from a liquefied layer, and then back to point C for drying process after earthquake shaking is shown by the broken line in Figure 1.

Coefficients of permeability of fluid and air assumed for this study are also based on van Genuchten (1980) as

$$\mathbf{k}^f = \mathbf{k}^f_{S_e=1}(S_e)^{n_{kf}}\left[1 - \left(1 - S_e^{\frac{1}{m_f}}\right)^{m_f}\right]^2, \ \mathbf{k}^a = \mathbf{k}^a_{S_e=0}(1 - S_e)^{n_{ka}}\left(1 - S_e^{\frac{1}{m_f}}\right)^{2m_f} \tag{18}$$

5 HORIZONTALLY LAYERED PARTIALLY SATURATED LIQUEFIABLE GROUND

The proposed formulation of governing equations of three phase medium is combined with the strain space multiple mechanism model for granular materials (Iai et al., 2011) for effective stress analysis of soil-structure systems consisting of partially saturated liquefiable ground. In the strain space multiple mechanism model, the effective stress, defined as extension positive, is given based on a dyad defined by the unit vector **n** along the direction of the branch between the particles in contact with each other and the unit vector **t** normal to **n** as follows:

$$\sigma' = -p\mathbf{I} + \frac{1}{4\pi}\int\int q\langle\mathbf{t}\otimes\mathbf{n}\rangle d\omega d\Omega, \ \langle\mathbf{t}\otimes\mathbf{n}\rangle = \mathbf{t}\otimes\mathbf{n} + \mathbf{n}\otimes\mathbf{t} \tag{19}$$

where p denotes effective confining pressure (compression positive), **I** denotes second order identity tensor, q denotes micromechanical stress contributions to macroscopic deviator stress due

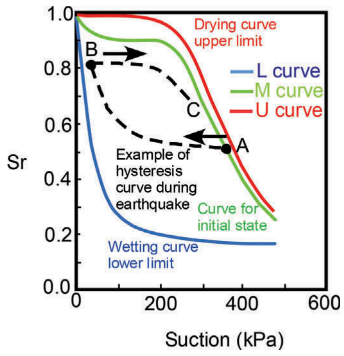

Figure 1. Soil-water retention characteristics (with parameters specified in Table 1)

Table 1. Parameters of soil-water retention characteristics and coefficient of permeability

soil-water retention characteristics (Eq.(17))							coefficient of permeability (Eq.(18))				
S_{rx}	S_{rn}	s_{aU}(kPa)	n_{fU}	s_{aL}(kPa)	n_{fL}	m_f	$k^{f}_{s_e=1}$ (m/s)	$k^{a}_{s_e=0}$ (m/s)	n_{k_f}	n_{k_a}	ε_k
0.99	0.15	358	5.9	29	1.45	1.0	1.0×10^{-4}	5.0×10^{-3}	0.5	0.5	1.0×10^{-4}

Conditions for initial gravity analysis stage: Adopting a middle curve going through a point with degree of saturation S_{ri}=0.9 and suction s_i=200kPa.

to virtual simple shear mechanism (called virtual simple shear stress), and $\langle \mathbf{t} \otimes \mathbf{n} \rangle$denotes second order tensor representing the virtual simples shear mechanism. In the double integration, the integration with respect to ω(=0 through π) is taken over a virtual plane spanned by the direction vectors **n** and **t** with $\omega/2$ being the angle of **n** relative to the reference local coordinate defined in the virtual plane, while the integration with respect to the solid angle Ω is taken over a surface of a unit sphere to give a three dimensional average of two dimensional mechanisms.

The integrated form of the constitutive equation, i.e. direct stress strain relationship, is derived by relating the macroscopic strain tensor $\boldsymbol{\varepsilon}$ to the macroscopic effective stress $\boldsymbol{\sigma}$' through the structure defined by Eq.(19). The first step to derive this relationship is to define the volumetric strain ε (extension positive) and the virtual simple shear strains $\boldsymbol{\gamma}$ as the projections of the macroscopic strain field to the second order tensors representing volumetric and virtual simple shear mechanisms as follows:

$$\varepsilon = \mathbf{I} : \varepsilon, \;\; \gamma = \langle \mathbf{t} \otimes \mathbf{n} \rangle : \boldsymbol{\varepsilon} \tag{20}$$

where the double dot symbol denotes double contraction. In order to take into account the effect of volumetric strain due to dilatancy ε_d, effective volumetric strain ε' is introduced by

$$\varepsilon' = \varepsilon - \varepsilon_d, \quad \dot{\varepsilon}_d = \mathbf{I}_d : \dot{\boldsymbol{\varepsilon}} \tag{21}$$

where the rate of volumetric strain due to dilatancy is given by the projection of strain rate field to a second order tensor $\mathbf{I}_d$.

The scalar variables defined in Eqs.(20) and (21) as the projection of macroscopic strain field are used to define the isotropic stress p and virtual simple shear stress q in Eq.(19) through path dependent functions as

$$p = p(\varepsilon'), \;\; q = q(\gamma) \tag{22}$$

In the strain space multiple mechanism model, the virtual simple shear mechanism is formulated as a non-linear hysteretic function, where a back-bone curve is given by the following hyperbolic function;

$$q(\gamma) = \frac{\gamma/\gamma_v}{1 + |\gamma/\gamma_v|} q_v \tag{23}$$

The parameters q_v and $\boldsymbol{\gamma}_v$ defining the hyperbolic function are the shear strength and the reference strain of the virtual simple shear mechanism, respectively.

The isotropic component in Eq.(22) is defined by a hysteretic tangential bulk modulus depending on the loading/unloading (L/U) condition as

$$K_{L/U} = -\frac{dp}{d\varepsilon'} = r_k K_{U0} \left(\frac{p}{p_0} \right)^{l_k} \tag{24}$$

where p_0: initial confining pressure, K_{U0}: tangential bulk modulus at initial confining pressure.

The first example of application of the proposed model is on horizontally layered partially saturated liquefiable ground based on one dimensional analysis. The ground consists of a uniform loose clean sand, 20m deep, with a ground water table located at a depth of 10m from ground surface. The parameters of strain space multiple mechanism model of sand used for the analysis are shown in Table 2 together with the parameters of pore water and air in Table 3. The parameters shown in Table 1 are used for representing soil-water retention characteristics and coefficient of permeability. For details of the parameters of the strain space multiple mechanism model shown in Table 2, refer to (Iai et al., 2011)

The analysis is performed in three stages: (1) 1st stage analysis is performed for computing degree of saturation based on M curve in Figure 1 with boundary conditions of pore water and air pressures set zero at the ground water table, (2) 2nd stage analysis is performed for initial static gravity analysis reflecting the initial degree of saturation and pore water and air pressures computed in the previous stage of analysis, and (3) 3rd stage analysis is performed for earthquake response analysis with boundary conditions of excess pore water and excess air pressures set zero at the ground surface with an input earthquake motion shown in Figure 2 assigned at the base of the ground at a depth of 20m. The analysis is performed with (Case-A) and without (Case-B) hysteresis in soil-water retention characteristics. The analysis is performed from 65s in Figure 2 as designated time zero in the computed results shown in Figure 3.

As shown in Figure 3, excess pore water pressure buildup below the ground water table induces pore water inflow into partially saturated layer above the ground water table, and degree of saturation in partially saturated layer gradually increases, resulting in the rise in the ground water table almost at 4m higher than the original ground water table.

In particular, pore air pressure rise in the vicinity of the ground water table is significant and dissipation of pore air pressure is significantly slower than that of excess pore water pressure. Suction is initially decreased in partially saturated layer due to pore water inflow from the layer below the ground water table, whereas suction is later increased in the vicinity of the ground water table probably due to the slower rate of dissipation of pore air pressure in these regions. Despite these increase in suction, degree of saturation is more or less steadily increased for Case-A (Figure 3(a)) whereas for Case-B (Figure 3(b)) degree of saturation is eventually back to the original level. This fact indicates that hysteresis in soil-water retention characteristics plays primary role in steady increase in degree of saturation and elevation of ground water table. The analysis suggests that the proposed analysis framework of partially saturated sand has the potential to simulate the steady increase of ground water table above the liquefiable sand layer.

6 AN EMBANKMENT WITH A PHREATIC LINE DURING EARTHQUAKE

The second example of application of the proposed model is on an embankment retaining water on one side with seepage flow subject to earthquake shaking based on two dimensional analysis. The embankment is 5m high founded on a foundation ground 5m deep, retaining water 4m deep as shown in Figure 5. The same model parameters shown in Tables 1 through 3 are used for the analysis, including the materials for the embankment and foundation ground, with the same input motion shown in Figure 2.

The analysis is performed in four stages: (1) 1st stage analysis is performed for computing degree of saturation based on M curve in Figure 1 with boundary conditions of pore water and air pressures set as shown in Figure 4, (2) 2nd stage analysis is performed for initial static gravity analysis by assuming no water is retained so that there is no seepage flow, (3) 3rd stage

Table 2. Parameters of strain space multiple mechanism model of sand for analysis

$K_{L/Ua}$ (kPa)	r_K	l_K	G_{ma} (kPa)	ϕ_f (°)	h_{max}	ϕ_p (°)	r_{ε_d}	$r_{\varepsilon_d^c}$	q_1	q_2	ε_d^{cm}	c_1
142400	0.5	2	54620	36.0	0.24	28.0	0.1	6.0	1.0	2.0	0.5	1.5

($p_a = 73.5$kPa, $r_\gamma = 0.1$, $S_1 = 0.005$)

Table 3. Parameters of pore water (fluid) and air for analysis

Density of soil (saturated) skeleton, fluid and air			bulk modulus of fluid and air		porosity
ρ (t/m^3)	ρ_f (t/m^3)	ρ_a (t/m^3)	K_f (kPa)	K_a (kPa)	n
2.1	1.0	1.23×10^{-3}	2.2×10^6	98	0.4

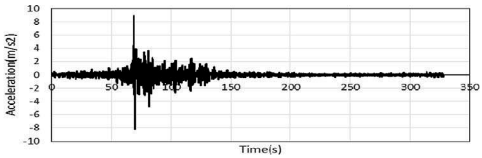

Figure 2. Input earthquake motion used for the analysis

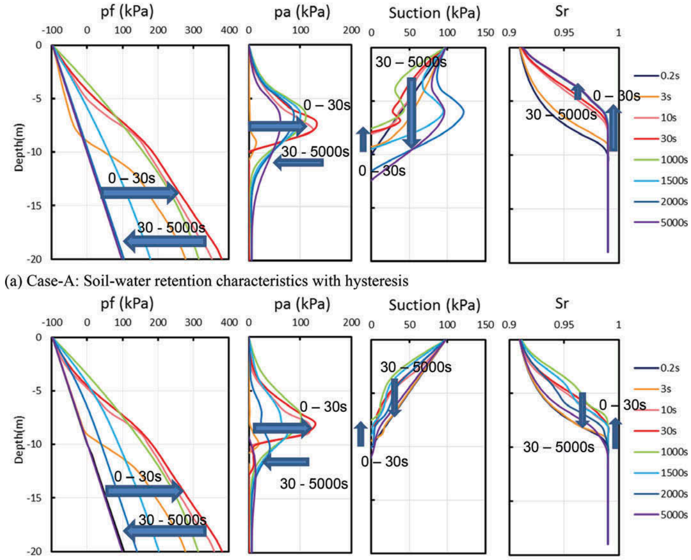

(a) Case-A: Soil-water retention characteristics with hysteresis

(b) Case-B: Soil-water retention characteristics without hysteresis

Figure 3. Computed pore water pressure (p_f), pore air pressure (p_a), suction and degree of saturation (S_r)

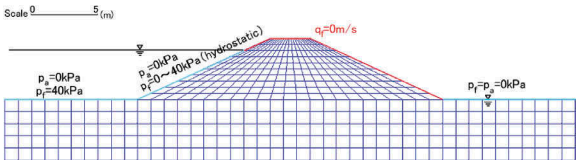

Figure 4. Cross section and specified boundary conditions on pore water and air pressures

analysis is reflecting the initial degree of saturation and pore water and air pressures computed in the 1st stage analysis, and (4) 4th stage analysis is performed for earthquake response analysis with boundary conditions of excess pore water and excess air pressures kept the same as shown in Figure 4.

As shown in Figure 5(a), computed results by the 1st stage analysis of seepage flow/phreatic line analysis indicate distribution of pore water pressures consistent with the pore water pressure distribution on the retaining surface of embankment and also consistent with the zero pressure boundary on the ground surface at the lower stream end. Computed phreatic line going through the embankment cross section inferred from the boundary between sky blue zone to dark blue zone is also consistent with those typical phreatic lines referred to in the literatures. Computed suction and degree of saturation shown in Figure 5(b)(c) also is consistent with the given boundary conditions of pore water and air pressures.

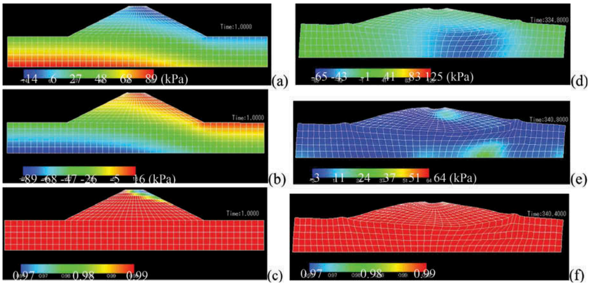

Figure 5. Computed results by seepage flow/phreatic line analysis before earthquake ((a) through (c)) and deformation at the end of earthquake response/liquefaction analysis ((d) through (f)): color contours indicate (a) pore water pressures, (b) suction, and (c) degree of saturation, (d) excess pore water pressures, (e) excess pore air pressures, and (f) degree of saturation

Computed deformation of embankment is shown in Figure 5 together with excess pore water and air pressures, and degree of suction. Excess pore water pressures indicate negative pressure zone in the downstream side probably due to dilative behavior associated with shear deformation towards downstream side as shown in Figure 5(d). There is a long delay in dissipation of pore air pressure as indicated by light blue color shown in Figure 5(e). Initially partially saturated zone above the inferred phreatic line is gradually going into fully saturated state as shown in Figure 5(f).

7 CONCLUSIONS

A new formulation of governing equation of three phase medium, consisting of solid skeleton, gas and water is proposed through a generalized fluid vector, which has significant advantage over conventional formulation when dealing with the increasing complexity in pore filling material such as mixtures of oil, water, air, natural gasses. Example analyses of this formation to earthquake response analysis of one and two dimensional analysis of partially saturated soil demonstrate the potential to simulate the steady increase of ground water table above the liquefiable sand layer and the deformation of partially saturated embankment on the liquefiable sand layer during earthquakes. In the next stage of study, validation of the proposed analysis framework with strain space multiple mechanism model will be expected through centrifuge model tests and investigation on case histories of seismic damage to partially saturated embankments.

REFERENCES

BORJA, R. I. 2004. Cam-Clay plasticity. Part V: A mathematical framework for three-phase deformation and strain localization analyses of partially saturated porous media. *Computer Methods in Applied Mechanics and Engineering*, 193, 5301–5338.

GENUCHTEN, V. 1980. A closed-form equation for predicting the hydraulic conductivity of unsaturated soils. *Soil Science Society of America Journal*, 44, 892–898.

IAI, S. 2018. Partially saturated soil: formulation through generalized fluid vector and validation with leaking test. *Geotechnical Earthquake Engineering and Soil Dynamics V*.

IAI, S., TOBITA, T., OZUTSUMI, O. & UEDA, K. 2011. Dilatancy of granular materials in a strain space multiple mechanism model. *International Journal for Numerical and Analytical Methods in Geomechanics*, 35, 360–392.

OHNO, S., IIZUKA, A. & OHTA, H. 2006. Two categories of new constitutive model derived from nonlinear description of soil contractancy. *Journal of Applied Mechanics, JSCE*, 9, 407–414 (in Japanese).

OZUTSUMI, O. 2003. *Numerical studies on soil-structure systems on liquefiable deposit during earthquakes*. Doctors Dissertation, Kyoto University, Japan.

ZIENKIEWICZ, O. C. & BETTESS, P. 1982. Soils and other saturated media under transient, dynamic conditions. *In*: PANDE & ZIENKIEWICZ (eds.) *Soil Mechanics - Transient and Cyclic Loads*. John Wiley and Sons.